Early deglaciation and paleolake history of the Río Cisnes Glacier,

Patagonian Ice Sheet 44°S

Supplementary information on the luminescence dating approach used in this study

Juan-Luis García[1*], Antonio Maldonado[2,3,4], María Eugenia de Porras[2,5], Amalia Nuevo Delaunay[6], Omar Reyes[7], Claudia A. Ebensperger[1], Steven A. Binnie[8], Christopher Lüthgens[9], César Méndez[6].**

1.-Instituto de Geografía, Facultad de Historia, Geografía y Ciencia Política, Pontificia Universidad Católica de Chile, Avenida Vicuña Mackenna 4860, Macul, Santiago, 782-0436, Chile.
2.- Centro de Estudios Avanzados en Zonas Áridas, La Serena, Chile.
3. Instituto de Investigación Multidisciplinario en Ciencia y Tecnología, Universidad de La Serena, la Serena, Chile.
4. Departamento de Biología Marina, Universidad Católica del Norte, Larrondo 281, Coquimbo, Chile.
5. Instituto Argentino de Nivología, Glaciología y Ciencias Ambientales (IANIGLA), CCT Mendoza CONICET, Av. Ruiz Leal s/n, Mendoza, Argentina
6.- Centro de Investigación en Ecosistemas de la Patagonia, Moraleda 16, Coyhaique, Chile.
7.- Centro de Estudios del Hombre Austral, Universidad de Magallanes, Punta Arenas, Chile.
8.- Institut für Geologie und Mineralogie, Universität zu Köln, Greinstraße 4-6, Gebäude 902, 50939, Köln, Germany.
9.- Institute for Applied Geology, University of Natural Resources and Life Sciences (BOKU), Vienna, Austria.

* Corresponding author. Phone #: 56-2-23544726; Fax #: 56-2-5526028. jgarciab@uc.cl
** Corresponding author for this supplement. Phone #: +4314765487213. christopher.luethgens@boku.ac.at

Introduction

This supplementary document provides detailed information about the luminescence dating approach applied in this study in addition to the basic information provided in the main text. All analytical steps described here were conducted at the Vienna Laboratory for Luminescence dating (VLL), including all sample preparation steps, gamma spectrometry measurements, luminescence analyses, and age calculation. For all stratigraphic, paleoclimatic, and geomorphological implications in the context of the extensive early deglaciation and paleolake history of the Río Cisnes Ice Lobe, Patagonia 44ºS, please see the text in the main paper.

Sample preparation

The luminescence samples were delivered to the VLL in closed, light-tight plastic cylinders. Additional sample material from the direct surroundings of the luminescence sampling spots was taken for radionuclide determination. All sample preparation was conducted at the VLL under subdued red-light conditions including mechanical, chemical, and density separation steps, to generate pure potassium-rich feldspar separates for all

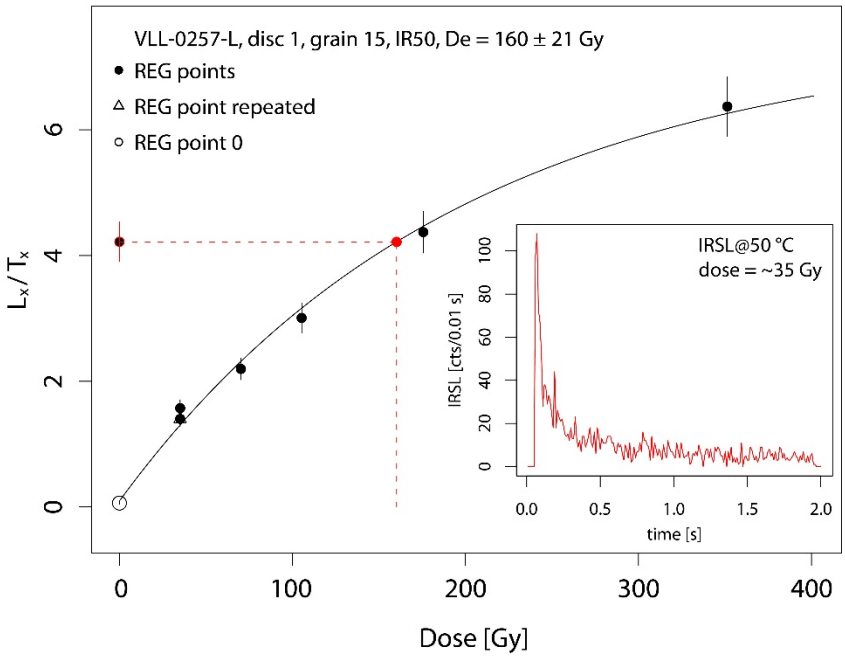

Supplementary figure L1: Representative dose response curve and decay curve for a single K-feldspar grain of sample VLL-0257-L. Plots generated using the R-luminescence package of Kreutzer et al. (2012).

samples. The detailed preparation steps are described in Lüthgens et al. (2017) and Rades et al. (2018).

Depending on the sample characteristics, the obtained grain sizes had to be adjusted between 100-300µm (see Table L1) to gain sufficient amounts of material for dating purposes. Detailed sample characteristics are provided in table L1. Samples for radionuclide determination were first dried and then stored in sealed Marinelli beakers (500ml equivalent to ~1kg dry weight of sample material) for at least four weeks, to establish secondary secular radon equilibrium.

Experimental setup

Determination of the equivalent dose

Potassium-rich feldspar was used for equivalent dose determination in this study. In contrast to quartz, feldspar frequently shows an athermal signal loss over time, termed anomalous fading (Wintle 1973), which has to be corrected for in age calculation to avoid age underestimation (e.g. Huntley & Lamothe 2001). Recently, new measurement protocols using a post infrared, infrared stimulated signal (pIRIR) from potassium-rich feldspar stimulated at higher temperatures were developed to circumvent fading correction by using a more stable luminescence signal (Buylaert et al. 2009, Buylaert et al. 2012). However, these pIRIR signals increase a general drawback of K-feldspar – its slow bleachability (e.g. Thiel et al. 2011). In depositional environments like the ones under investigation here (fluvial to glaciofluvial, waterlain sediments, short transport distances) incomplete bleaching was shown to be an issue in previous studies (e.g. Bickel et al. 2015a/b, Lüthgens et al. 2011, Rades et al. 2018, Thrasher et al. 2009, Wallinga 2002).

To find out whether incomplete bleaching was significant in our samples, we compared IR luminescence signals stimulated at different temperatures (Murray et al. 2012, Buylaert et

al. 2013). In the case of incomplete bleaching, a sample is expected to show increasing ages when comparing ages based on equivalent doses determined at lower temperatures with those determined at higher temperatures. In addition, the ages need to be corrected for fading for this comparison. We therefore measured a test sample using the infrared signal stimulated at 50°C (IR50), and the pIRIR signals stimulated at 150°C (pIRIR150), and 225°C (pIRIR225) using aliquots with a diameter of 1mm, each containing about 50 grains. The applied single aliquot regenerative (SAR) dose protocols successfully passed dose recovery tests, proving their suitability for the samples under investigation. In addition, fading tests were conducted for that sample using the approach of Auclair et al. (2003), but modified to also detect the pIRIR signals. The results showed a stimulation temperature dependent rising trend in apparent ages for the test sample, which clearly indicates incomplete bleaching to be present in the sample.

For K-feldspar, intense signal averaging (e.g. Reimann et al. 2012) prevents coping with this issue when using multigrain aliquots. Consequently, a single grain approach was adopted for all further measurements, using the IR50 signal, which is expected to be the most easily bleachable K-feldspar signal (Blomdin et al. 2012). All measurements were conducted in the VLL using a Risø DA-20 automated luminescence reader sytem equipped with a dual laser single grain system (Bøtter-Jensen et al. 2000, 2003).

Luminescence signals were stimulated using an 830nm IR laser and were detected through a LOT/Oriel D410/30 optical interference filter, selecting the K-feldspar emission at 410 nm (Krbetschek et al. 1997). The single grain IR50 SAR protocol successfully passed dose recovery tests for all samples (Table L1). A representative single grain growth curve and decay curve are shown in Fig. L1. Fading tests according to Auclair et al. (2003) were conducted using multigrain aliquots (following Blomdin et al. 2012) for all samples. The resulting g-values are summarised in Supplementary table 1.

Supplementary table L1: Luminescence sample properties and pre-tests

Sample codes		Position (decimal degrees, WGS 84)		Alti-tude (m)	Depth (m)	Grain size (µm)	Dose recovery ratios[1]	Dose recovery σb[3] (%)	g-value IR50[2]
laboratory	field	latitude	longitude						
VLL-0235-L	CIS-1501	-44.68222	-71.96872	550	1.2	200-250	1.1 ±0.3	14 ±2	3.9 ±0.9
VLL-0236-L	BER-1502	-44.59871	-71.43511	867	0.5	100-300	1.1 ±0.4	19 ±3	3.8 ±1.0
VLL-0237-L	CIS-1503	-44.68222	-71.96872	550	4.7	200-250	n/a	n/a	3.6 ±0.9
VLL-0238-L	CIS-1504	-44.56954	-71.24132	830	0.8	150-250	n/a	n/a	1.9 ±0.8
VLL-0239-L	CAR-1501	-44.51686	-71.46572	1006	0.9	100-300	1.1 ±0.4	28 ±3	3.8 ±0.7
VLL-0255-L	CIS-1601	-44.71527	-72.13062	311	1.6	100-300	n/a	n/a	3.6 ±0.7
VLL-0256-L	CIS-1602b	-44.71632	-72.13159	294	3.0	200-300	n/a	n/a	3.5 ±0.7
VLL-0257-L	CIS-1603b	-44.71636	-72.12695	285	6.0	200-250	0.9 ±0.3	18 ±2	2.7 ±0.8

[1] Measured 300 grains per sample with 100-200 grains passing the rejection criteria.

[2] Determined as arithmetic mean ± standard deviation, using 6 aliquots per sample.

[3] Overdispersion (σ_b) calculated using the Central Age Model (CAM) of Galbraith et al. (1999)

Determination of the dose rate

By using high resolution, low level gamma spectrometry, the content of naturally occurring radionuclides (^{238}U and ^{232}Th decay chains, as well as ^{40}K) contributing to the external doserate was determined. To achieve a preferable signal to noise ratio, each sample was measured for 24 hours at the VLL using a Canberra HPGe (40 % n-type) detector. Based on the results from radionuclide analysis (Supplementary table 2), the external dose rate was calculated using the conversion factors of Adamiec & Aitken (1998) and the β-attenuation factors of Mejdahl (1979). An average water content of 15 ±5 % was estimated for the time of burial. The resulting water content range of 10-20 percent therefore covers almost dry to almost saturated conditions. Higher water content values would result in more effective shielding of ionising radiation within the sediment, and would therefore result in lower doserates and consequently in higher ages. As the water content values have to represent the average water content in the sediment since burial, a large range of uncertainty was assigned to the water content (15 ±5 %), which was propagated to the final doserate and age calculation. In addition, an average alpha efficiency (a-value) of 0.08 ±0.01, as well as an average internal potassium content of 12.5 ±0.5% (following Huntley & Baril 1997) was also taken into account for doserate calculation. The cosmic doserate was determined according to Prescott & Stephan (1982) and Prescott & Hutton (1994), taking the geographical position of the sampling spot (longitude, latitude, and altitude), the depth below surface, as well as the average density of the sediment overburden into account. An uncertainty of 10% was assigned to the calculated cosmic doserate.

Supplementary table L2: Results from radionuclide analysis and dose rate calculation

Sample lab code	Sample field code	^{238}U (ppm)	^{232}Th (ppm)	K (%)	Water content (%)[1]	Cosmic doserate (Gy/ka)	External + internal doserate Fs (Gy/ka)[2]
VLL-0235-L	CIS-1501	1.20 ±0.03	4.28 ±0.16	1.90 ±0.04	15 ±5	0.20 ±0.02	2.87 ±0.16
VLL-0236-L	BER-1502	2.15 ±0.05	9.36 ±0.33	2.52 ±0.05	15 ±5	0.23 ±0.02	3.86 ±0.23
VLL-0237-L	CIS-1503	1.19 ±0.03	4.81 ±0.15	1.84 ±0.04	15 ±5	0.13 ±0.01	2.85 ±0.15
VLL-0238-L	CIS-1504	1.36 ±0.04	5.44 ±0.20	1.87 ±0.04	15 ±5	0.22 ±0.02	2.88 ±0.16
VLL-0239-L	CAR-1501	1.86 ±0.05	8.14 ±0.23	2.09 ±0.05	15 ±5	0.23 ±0.02	3.36 ±0.20
VLL-0255-L	CIS-1601	1.72 ±0.04	7.53 ±0.21	2.13 ±0.05	15 ±5	0.18 ±0.02	3.33 ±0.19
VLL-0256-L	CIS-1602b	1.00 ±0.02	4.14 ±0.15	1.41 ±0.03	15 ±5	0.15 ±0.02	2.50 ±0.13
VLL-0257-L	CIS-1603b	1.38 ±0.04	5.81 ±0.21	2.03 ±0.04	15 ±5	0.10 ±0.01	3.21 ±0.18

[1] Estimated average water content throughout burial time. Values covering almost dry to almost saturated conditions. Error was propagated to the overall doserate calculation.

[2] Including an alpha attenuation factor of 0.08 ±0.01 and an internal K content of 12.5 ±0.5%.

Results

Based on the results from dose recovery experiments, data evaluation of the SAR single grain measurements was carried out using the following rejection criteria: recycling <20%, recuperation <20% of the natural signal, test dose error <20%, and signal >3σ above background. Three of the equivalent dose distributions show rather narrow, normal distributions with rather low overdispersion values ranging around 25-35% (Tab. L3, Fig. L1). These overdispersion values are only slightly higher than those achieved in dose recovery

experiments (Tab. L1), which represent the lowest achievable spread in data to be expected. Therefore, we consider these samples to have been fully bleached prior to deposition. The central age model (CAM) of Galbraith et al. (1999) was used for the calculation of average equivalent doses for these samples. The other samples, however, show broad, positively skewed dose distributions characterised by rather high overdispersion values (between 50-90 %) as expected from incompletely bleached samples (Supplementary table L3, Supplementary figure L2). To take this into account in equivalent dose calculations, the three parameter minimum age model (MAM, Galbraith et al. 1999) was applied for the calculation of equivalent dose values for these samples. A threshold value of 0.3 (30%) for σ_b (defining the minimum expected scatter) was chosen based on the maximum overdispersion values observed for well bleached samples. The resulting equivalent doses are summarised in Supplementary table L3. Age calculation was conducted using the software ADELE (Kulig 2005). The resulting ages were then corrected for fading based on the approach of Huntley & Lamothe (2001) and using the g-values determined for the individual samples (supplementary Tab. L1). All calculations apart from doserate and age calculations were done using the R-Luminescence package of Kreutzer et al. 2012. Supplementary table L3 shows a summary of the results.

Reliability of the data

By applying the chosen single grain Fs SAR approach for determination of the equivalent dose, it was possible to reliably identify incompletely bleached samples in the dataset. Based on the maximum overdispersion value observed from the well bleached samples, the threshold value of σ_b for use in the MAM calculations could be determined directly from the dataset. The resulting ages were subsequently corrected for fading and show consistent results with respect to their relative stratigraphical position. At two sites, age control is available from independent methods. At the Antena Site, samples CIS-1501 (11.0 ±1.8 ka) and CIS-1503 (10.5 ±1.7 ka) are in good agreement within error and bracket a radiocarbon date providing a maximum age of deposition of 12.7 ±0.07 ka Cal BP, which is within error in excellent agreement with the ages calculated for both samples. At the Las Barrancas Site, sample CIS-1504 yielded an age of 19.5 ±3.0 ka which perfectly agrees with the maximum calibtrated ^{14}C age of sediments deposited at 19.8 ±0.2 ka Cal BP (CIS-414-4).

Based on the successful comparison between these two independent dating methods, we argue that the chosen experimental setup, as well as the statistical approaches used for equivalent dose calculations for both, well bleached and poorly bleached samples are reliable. From a methodological point of view we therefore interpret the obtained luminescence ages to be reliable for all but one sample. For that one sample, CAR-1501, the dataset is rather limited, owing to the minimal amount of suitable material available for sample preparation and for measurement of that sample. The sample characteristics qualify this sample as incompletely bleached; however, the limited dataset prevents a thorough statistical analysis using the MAM-3. We therefore interpret the age of sample CAR-1501as a maximum age, in other words, deposition happened sometime after <38.3 ±6.4 ka.

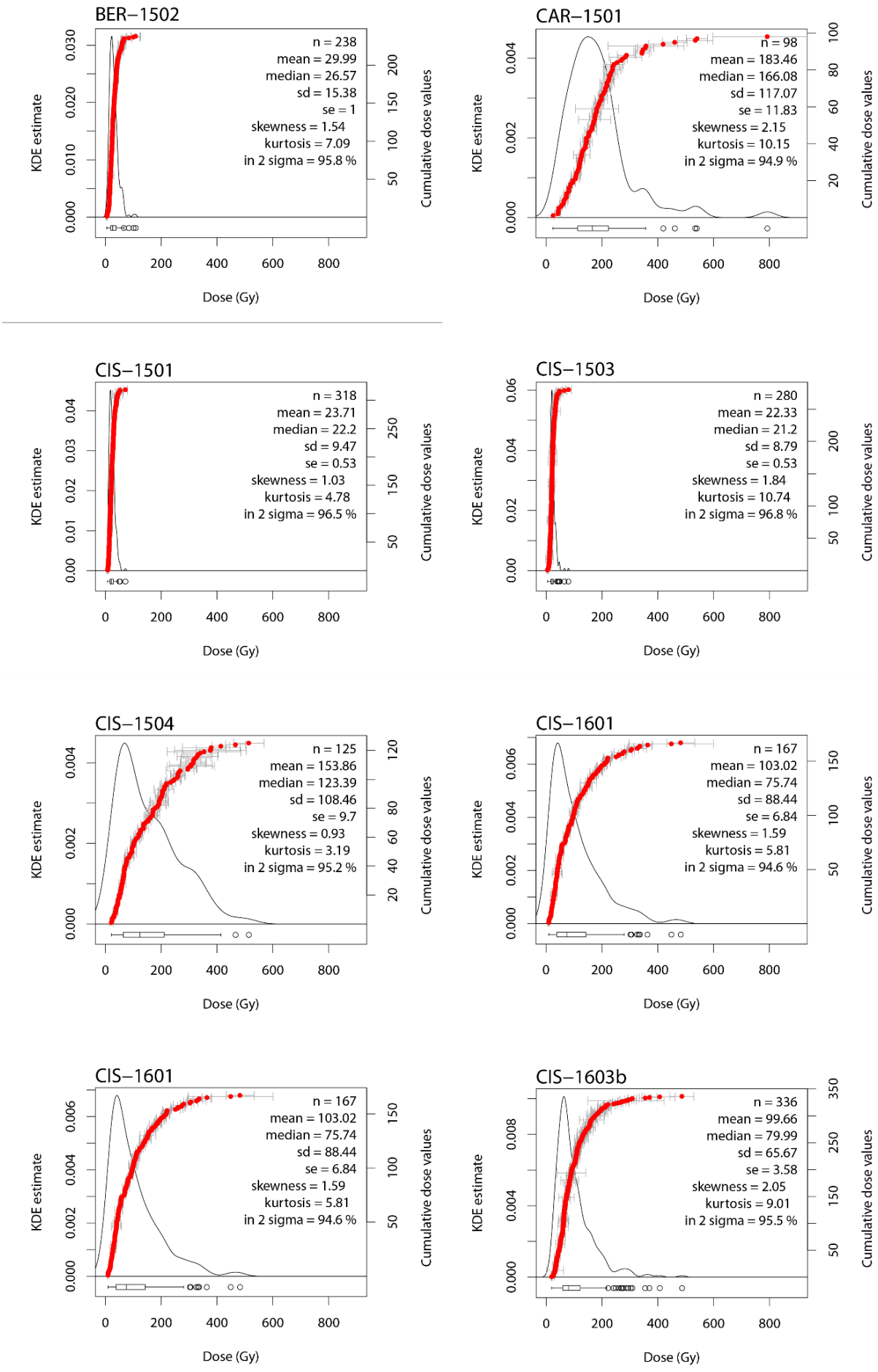

Supplementary figure L2: Equivalent dose distributions for all samples under investigation. KDE-plots generated using the R-luminescence package of Kreutzer et al. (2012).

For single grain feldspar dating, the internal potassium content of the individual grains contributes a significant portion to the overall doserate. Inter-grain variations in K-content may therefore influence the dating results. To circumvent this issue, it has been proposed to only use the brightest proportion of grains for age calculation (e.g. Smedley et al. 2016), because it most likely represents end members of K-feldspar with a similar average K-content. For some of our samples only very limited amounts of material were available in a suitable grainsize for single grain dating techniques. For one sample only <100 equivalent dose values passed all rejection criteria. However, we still tested the "brightest grains" approach, using the brightest 30% of grains (determined from the first test dose response) for all equivalent dose measurements and dose-recovery tests. For all dose recovery tests and the majority of equivalent dose determinations (those with a sufficiently large dataset of at least about 100 equivalent dose values), a significant change of the resulting equivalent doses was not observed. Because of that and because of the fact that our calculations including all values are in agreement with age control from an independent method, we conclude that using the "brightest grains" approach is not necessary here. Rades et al. (2018) present similar results in a recent study dealing with glaciofluvial sediments from the European Alps. The overall results from our single grain K-feldspar dating approach are summarised in Supplementary table L3, which is also included in the main paper (Table 4). For the interpretation of the luminescence ages in their geomorphological and stratigraphical context, we refer to the main text of this study.

Supplementary table L3: Summary of OSL data (This table is also presented in the main paper as Table 4, but is reprinted here for completeness of this supplementary document.)

Sample lab code	Sample field code	Fs SG (n)[1]	σb[2] (%)	Fs IRSL50 D_e (Gy)[3]	Dose rate Fs (Gy/ ka)[4]	Fs IR50 age (ka) faded[5]	Fs IR50 age (ka) fading corr.[6]
VLL-0235-L	CIS-1501	318	31 ±2	23.1 ±0.5	3.07 ±0.18	7.5 ±0.8	**11.0 ±1.8**
VLL-0236-L	BER-1502	238	35 ±3	28.6 ±0.8	4.09 ±0.25	7.0 ±0.8	**10.1 ±1.9**
VLL-0237-L	CIS-1503	280	24 ±2	22.0 ±0.5	2.98 ±0.16	7.4 ±0.8	**10.5 ±1.7**
VLL-0238-L	CIS-1504	125	69 ±5	50.7 ±5.8	3.10 ±0.18	16.3 ±2.1	**19.5 ±3.0**
VLL-0239-L	CAR-1501	98	52 ±4	91.9 ±10.4	3.59 ±0.22	25.6 ±3.3	**<38.3 ±6.4***
VLL-0255-L	CIS-1601	167	81 ±5	27.4 ±3.1	3.51 ±0.21	7.8 ±1.1	**11.1 ±1.8**
VLL-0256-L	CIS-1602b	157	79 ±5	26.8 ±2.9	2.65 ±0.15	10.1 ±1.2	**14.3 ±2.2**
VLL-0257-L	CIS-1603b	336	54 ±2	48.5 ±3.9	3.31 ±0.19	15.1 ±1.5	**19.6 ±2.6**

[1] Number of grains passing all rejection criteria.
[2] Overdispersion calculated using the CAM (Galbraith et al. 1999)
[3] Calculated using the CAM (Galbraith et al. 1999) for samples CIS-1501, BER-1502, CIS-15-03. All other samples calculated using the MAM-3 (Galbraith et al. 1999) with a threshold value of 0.3 for σb.
[4] Overall doserate. Details please see Table L2.
[5] Ages calculated using the software ADELE (Kulig 2005).
[6] Fs based ages corrected for fading according to the method of Huntley & Lamothe (2001) using the R Luminescence package (Kreutzer et al. 2012). These ages are printed in bold characters, because they are used for all subsequent interpretation.
* This age must be interpreted as a maximum age.

References

Adamiec, G., Aitken, M., 1998. Dose-rate conversion factors: update. Ancient TL 16, 37-50.

Auclair, M., Lamothe, M., Huot, S., 2003. Measurement of anomalous fading for feldspar IRSL using SAR. Radiation Measurements 37, 487-492.

Blomdin, R., Murray, A., Thomsen, K., Buylaert, J.-P., Sohbati, R., Jansson, K., Alexanderson, H., 2012. Timing of the deglaciation in southern Patagonia: Testing the applicability of K-Feldspar IRSL. Quaternary Geochronology 10, 264-272.

Bickel, L., Lüthgens, C., Lomax, J., Fiebig, M., 2015a. Luminescence dating of glaciofluvial deposits linked to the penultimate glaciation in the Eastern Alps. Quaternary International 357, 110-124.

Bickel, L., Lüthgens, C., Lomax, J., Fiebig, M., 2015b. The timing of the penultimate glaciation in the northern Alpine Foreland: new insights from luminescence dating. Proceedings of the Geologists' Association 126, 536-550.

Bøtter-Jensen, L., Andersen, C., Duller, G., Murray, A., 2003. Developments in radiation, stimulation and observation facilities in luminescence measurements. Radiation Measurements 37, 535-541.

Bøtter-Jensen, L., Bulur, E., Duller, G., Murray, A., 2000. Advances in luminescence instrument systems. Radiation Measurements 32, 523-528.

Buylaert, J., Murray, A., Thomsen, K., Jain, M., 2009. Testing the potential of an elevated temperature IRSL signal from K-feldspar. Radiation Measurements 44, 560-565.

Buylaert, J., Jain, M., Murray, A., Thomsen, K., Thiel, C., Sohbati, R., 2012. A robust feldspar luminescence dating method for Middle and Late Pleistocene sediments. Boreas 41, 435-451.

Buylaert, J., Murray, A., Gebhardt, A., Sohbati, R., Ohlendorf, C., Thiel C., Wastegård, S., Zolitschka, B., 2013. Luminescence dating of the PASADO core 5022-1D from Laguna Potrok Aike (Argentina) using IRSL signals from feldspar. Quaternary Science Reviews 71, 70-80.

Duller, G.A.T., 2006. Single grain optical dating of glacigenic deposits. Quaternary Geochronology 1, 296-304.

Galbraith, R., Roberts, R., Laslett, G., Yoshida, H., Olley, J., 1999. Optical dating of single and multiple grains of Quartz from Jinmium rock shelter, northern Australia: Part I, experimental design and statistical models. Archaeometry 41, 339-364.

Glasser, N., Harrison, S., Ivy-Ochs, S., Duller, G., Kubik, P., 2006. Evidence from the Rio Bayo valley on the extent of the north Patagonian ice field during the late Pleistocene – Holocene transition. Quaternary Research, 65, 70-77.

Glasser, N., Jansson, K., Duller, G., Singarayer, J., Holloway, M., Harrison, S., 2016. Glacial lake drainage in Patagonia (13-8 kyr) and response of the adjacent Pacific Ocean. Scientific Reports 6, 1-7.

Harrison, S., Glasser, N., Winchester, V., Haresign, E., Warren, C., Duller, G., Bailey, R., Ivy-Ochs, S., Jansson, P., Kubik, P., 2008. Glaciar León, Chilean Patagonia: late-Holocene chronology and geomorphology. The Holocene 18, 643-652.

Huntley, D., Baril, M., 1997. The K content of the K-feldspars being measured in optical and thermoluminescence dating. Ancient TL 15, 11-13.

Huntley, D., Lamothe, M., 2001. Ubiquity of anomalous fading in K-feldspars and the measurement and correction for it in optical dating. Canadian Journal of Earth Sciences 38, 1093-1106.

Krbetschek, M., Götze, J., Dietrich, A., Trautmann, T., 1997. Spectral information from minerals relevant for luminescence dating. Radiation Measurements 27, 695-748.

Kreutzer, S., Schmidt, C., Fuchs, M., Dietze, M., Fuchs, M., 2012. Introducing an R package for luminescence dating analysis. Ancient TL 30, 1-8.

Kulig G., 2005. Erstellung einer Auswertesoftware zur Altersbestimmung mittels Lumineszenzverfahren unter spezieller Berücksichtigung des Einflusses radioaktiver Ungleichgewichte in der ^{238}U-Zerfallsreihe. 35 p., B.Sc. thesis, Freiberg (Technische Universität Bergakademie Freiberg).

Lüthgens, C., Neuhuber, S., Grupe, S., Payer, T., Peresson, M., Fiebig, M., 2017. Geochronological investigations using a combination of luminescence and cosmogenic nuclide burial dating of drill cores from the Vienna Basin. Zeitschrift der Deutschen Gesellschaft für Geowissenschaften 168, 115-140.

Lüthgens, C., Böse, M., Preusser, F., 2011. Age of the Pomeranian ice marginal position in north-eastern Germany determined by Optically Stimulated Luminescence (OSL) dating of glaciofluvial (sandur) sediments. Boreas 40, 598-615.

Mejdahl, V., 1979. Thermoluminescence dating: beta attenuation in quartz grains. Achaeometry 21, 61-73.

Murray, A., Thomsen, K., Masuda, N., Buylaert, J., Jain, M., 2012. Identifying well-bleached quartz using the different bleaching rates of quartz and feldspar luminescence signals. Radiation Measurements 47, 688-695.

Preusser, F., Degering, D., Fuchs, M., Hilgers, A., Kadereit, A., Klasen, N., Krbetschek, M., Richter, D. & Spencer, J., 2008. Luminescence dating: basics, methods and applications. E&G Quaternary Science Journal, 57, 95-149.

Prescott, J., Hutton J., 1994. Cosmic ray distributions to dose rates for luminescence and ESR dating: large depths and long-term variations. Radiation Measurements 23, 497-500.

Prescott, J., Stephan, L., 1982. The contribution of cosmic radiation to the environmental dose for thermoluminescent

dating - Latitude, altitude and depth dependencies. PACT 6, 17-25.

Rades, E., Fiebig, M., Lüthgens, C., 2017. Luminescence dating of the Rissian type section in southern Germany as a base for correlation. Quaternary International, 478, 38-50.

Reimann, T., Thomsen, K., Jain, M., Murray, A., Frechen, M., 2012, Single-grain dating of young sediments using the pIRIR signal from feldspar. Quaternary Geochronology 11, 28-41.

Rhodes, E., 2011. Optically Stimulated Luminescence Dating of Sediments over the Past 200,000 Annual Review of Earth and Planetary Sciences 39, 461-488.

Smedley, R., Glasser, N., Duller, G., 2016. Luminescence dating of glacial advances at Lago Buenos Aires (~46 °S), Patagonia. Quaternary Science Reviews 134, 59-73.

Thrasher, I., Mauz, B., Chiverrell, B., Lang, A., 2009. Luminescence dating of glaciofluvial deposits: a review. Earth Science Reviews 97, 133-146.

Thiel, C., Buylaert, J., Murray, A., Terhorst, B., Hofer, I., Tsukamoto, S., Frechen, M., 2011. Luminescence dating of the Stratzing loess profile (Austria) – Testing the potential of an elevated temperature post-IR IRSL protocol. Quaternary International 234, 23-31.

Wallinga, J., 2002. On the detection of OSL age overestimation using single-aliquot techniques. Geochronometria 21, 17-26.

Wintle, A., 1973. Anomalous Fading of Thermo-luminescence in Mineral Samples. Nature 245, 143-144.

Wintle, A., 2008. Luminescence dating: where it has been and where it is going. Boreas 37, 471-482.